Z. Phys. Chem. **217** (2003) 447–458

Spontaneous and Electrodeposition of Pt on Ru(0001)

By M. S. Zei*, T. Lei, and G. Ertl

Fritz-Haber-Institut der Max-Planck-Gesellschaft, Faradayweg 4–6, D-14195 Berlin, Germany

Dedicated to Prof. Dr. Dieter M. Kolb on the occasion of his 60th birthday

(Received September 16, 2002; accepted in revised form October 15, 2002)

Ruthenium / Spontaneous Pt Deposition / Methanol Electrooxidation / RHEED / SEM

Pt was deposited onto a Ru(0001) electrode from a $PtCl_6^{2-}$-containing $HClO_4$ solution either electrochemically or spontaneously (*i.e.* without external current flow). Composition, structure and morphology of the deposit were studied by means of Auger electron spectroscopy (AES), high energy electron diffraction (RHEED), and scanning electron microscopy (SEM). At first pseudomorphic growth of a 2D-Pt adlayer takes place, while with higher coverages 3D-clusters develop for which the most densely packed [011]-rows of the Pt(111) planes are parallel with the most densely packed [1120]-rows of the Ru(0001) substrate. These Pt-clusters exhibit typical diameters between 2 and 10 nm, while their average mutual separation varies with the total amount of deposit. If compared with the bare Ru(0001) surface, the samples with Pt deposits exhibit considerably enhanced activity with respect to electrooxidation of formic acid or methanol.

1. Introduction

Deposition of a metal A on a substrate B enables the preparation of materials with particular chemical properties, which may, among others, serve as model systems for electrocatalysis [1–3]. Apart from evaporation also deposition from electrolyte solution, either spontaneously or electrochemically, may be applied. The spontaneous technique has *e.g.* be used for preparing Ru-modified Pt(111) [4, 5] as well as Pt/Ru(0001) surfaces [6]. Remarkable enhancements of the electrocatalytic activity towards methanol and formic acid oxidation has been found with both Ru- [7, 8] and Pd-modified [9, 10] Pt electrodes. The

* Corresponding author. E-mail: zei@fhi-berlin.de

present paper describes the formation and characterization of surfaces of the opposite combination, namely Ru(0001) electrodes partly covered by Pt.

2. Experimental

The experiments were performed with an apparatus consisting of a UHV chamber (base pressure $< 1.5 \times 10^{-10}$ mbar) incorporating LEED, RHEED and AES, an electrochemical chamber (base pressure $< 1.0 \times 10^{-9}$ mbar), an electrochemical cell and a closed sample transfer. The electrochemical cell consists of two parts, and a flow-cell procedure has been used which allows us to change electrolyte solutions under potential control and in an air-free atmosphere.

RHEED was performed with an incident electron beam (40 keV) at a grazing angle of 1–2° to the surface. The RHEED electron beam also acts as the primary electron source for AES. This combination allows RHEED and AES data to be recorded from the same surface region, thus correlating the structure and chemical composition data.

The working electrode, a Ru(0001) single crystal disc of 7 mm diameter and 2 mm thickness, was mounted between tungsten wires which also served for resistive heating of the sample. The electrode surface was prepared by cycles of argon ion bombardments (5×10^{-5} mbar, at room temperature and 700 °C), until the sample surface was free from disorder and impurities as controlled by LEED/RHEED and AES. The sample was then transferred to the electrochemical chamber under UHV conditions where the reactivity was probed by cyclic voltammetry (CV) for which the electrolyte forms a meniscus on top of a glass capillary through which the electrolyte is filled by argon gas and then the working electrode is brought into contact with the meniscus by movement of the glass capillary [11]. Standard electrochemical equipment was employed for potential sweeping. The electrode surface was again characterized after the electrochemical treatments and emersion by LEED/RHEED and AES. The experimental details have been reported elsewhere [11, 12].

A platinum wire with 0.4 mm diameter was used as counter electrode in the electrolyte vessel on top of a glass capillary [11]. In order to check the cleanliness of the Ru electrode the cyclic voltammogram for the clean Ru(0001) electrode was first recorded in a 0.1 M $HClO_4$ solution prior to Pt deposition.

Spontaneous deposition of Pt on the Ru(0001) surface was achieved by immersing the electrode for various periods of time into a 0.1 M $HClO_4$ solution containing 0.1 mM H_2PtCl_6, while electrochemical deposition was performed by cycling the potential between -0.2 and $+0.3$ V *vs.* Ag/AgCl. After finishing an experiment the sample was removed from the UHV system and polished with 0.02 μm alumina followed by careful rinsing with Millipore water.

3. Results and discussion

The structure of the Pt modified Ru(0001) surface was analyzed by high energy electron diffraction (RHEED). Fig. 1 shows the Ewald sphere construction for RHEED where the 2D-reciprocal lattice rods (RLR) for two Laue zones, L_0 and L_1, are marked by full and broken lines, respectively. Diffraction beams are created whenever the Ewald sphere intersects the RLRs. A clean and well ordered Ru(0001) surface (formed by argon ion sputtering and subsequent annealing) gives rise to a (1×1) RHEED pattern as reproduced in Figs. 2a and 2b. The (10) reflection corresponds to the reciprocal lattice vector a_1^* of the Ru(0001) surface, while the (11) reflection corresponds to $a_1^* + a_2^*$. The geometry of the reciprocal lattice together with the real lattice is illustrated by Fig. 3.

Representative RHEED patterns from a Pt covered Ru(0001) surface are reproduced in Figs. 2c and 2d. This sample was prepared by spontaneous de-

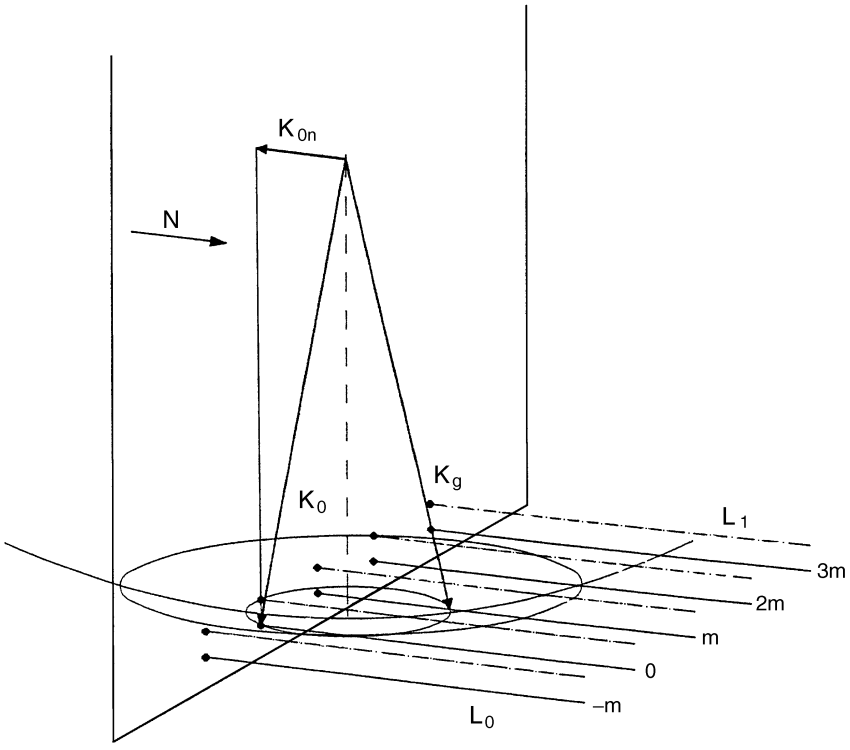

Fig. 1. Ewald sphere construction for high energy electron diffraction (RHEED) where the 2D-reciprocal lattice rods indicated by the solid and dashed lines intersect the Ewald sphere at zero Laue-L_0 and first Laue-zone L_1, respectively. $\boldsymbol{K}_0$ and $\boldsymbol{K}_g$ are the wave vectors of the incident and the diffracted electron beams, respectively.

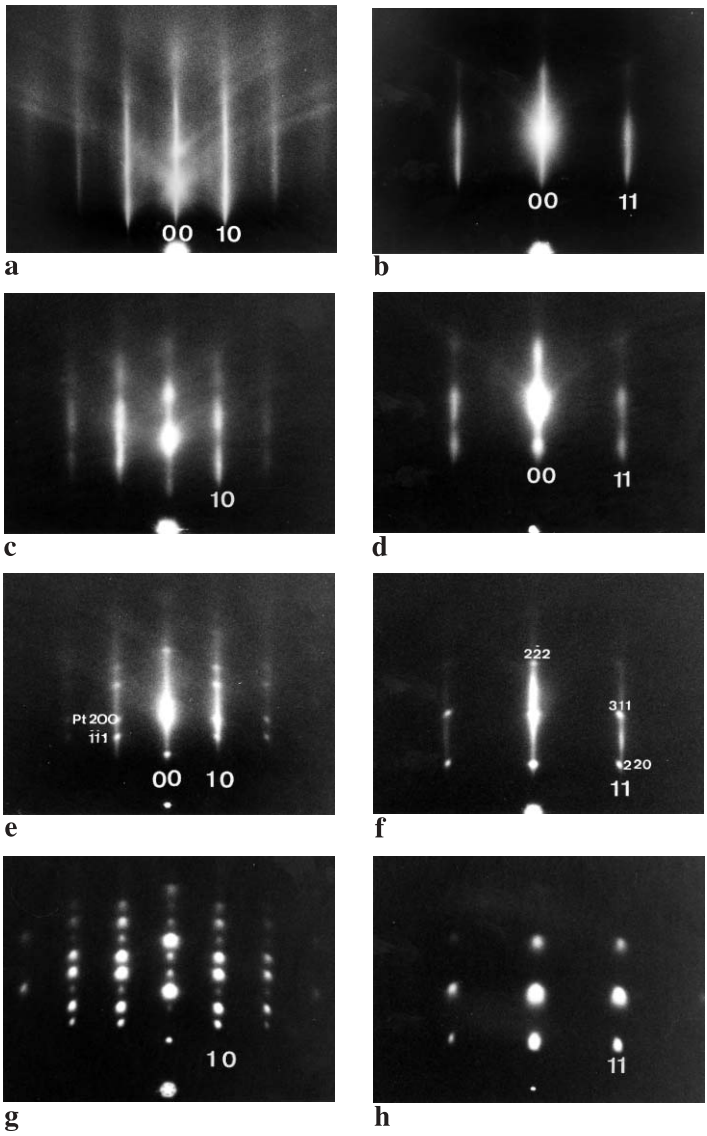

Fig. 2. (1×1) RHEED patterns ([1120] (a) and [0110] (b)) for Ru(0001) after argon ion sputtering and annealing under UHV conditions, showing 2D reflection streaks of (10) and (11) beams; RHEED patterns ([1120] (c) and [0110] (d)) for Ru(0001) electrode covered by 2D Pt-adlayer, showing intensity modulation along the (10) and (11) reflections; RHEED patterns ([1120] (e) and [0110] (f)) for the Ru(0001) electrode covered by Pt clusters which was obtained by spontaneous Pt deposition, showing 3D reflection spots besides the (10) and (11) reflection streaks; RHEED patterns ([1120] (g) and [0110] (h)) for the Ru(0001) electrode covered by 3D Pt clusters which was obtained by electrodeposition of Pt onto Ru(0001), showing only 3D reflection spots.

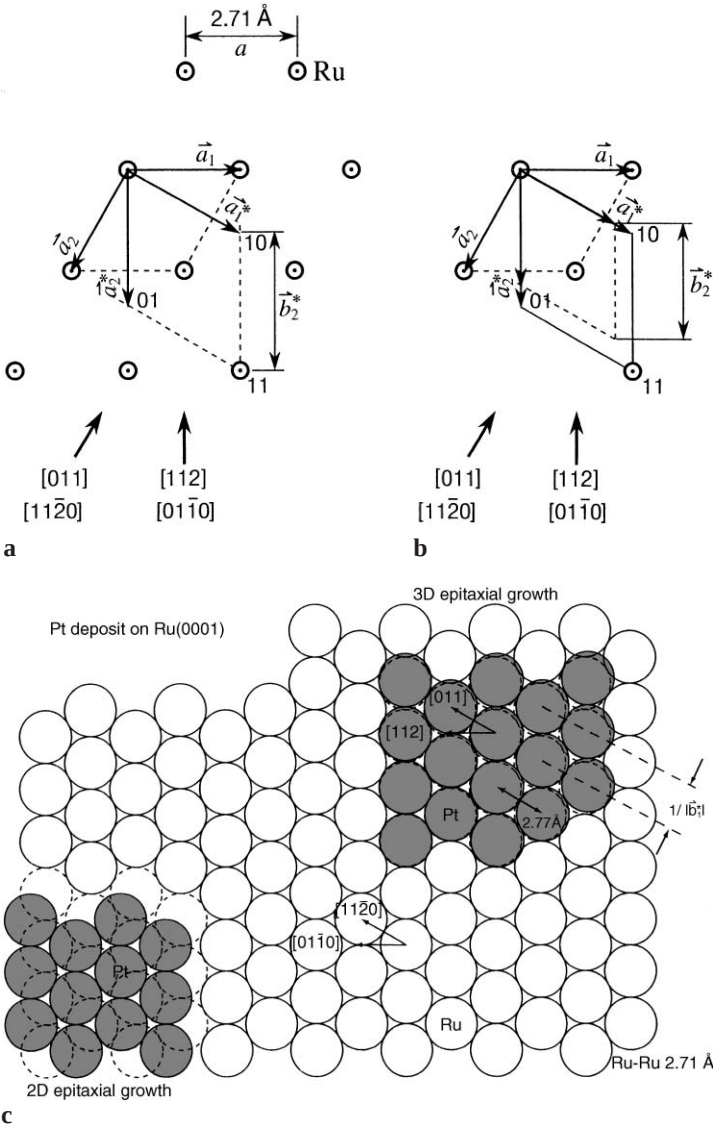

Fig. 3. (a) Two-dimensional (2D) hcp reciprocal lattice of a hexagonal Ru(0001) surface where a_1 and a_2 are the unit vectors of a hexagonal unit mesh of Ru(0001) and a_1^*, a_2^* are the corresponding reciprocal vectors ($a_1^* \perp a_2$ and $a_2^* \perp a_1$). b_1^*, b_2^* denote the reciprocal lattice vectors of a Pt adlayer. The reciprocal unit mesh of the Pt-adlayer coincides with the reciprocal unit mesh of the Ru substrate, (b) 2D hcp reciprocal lattice of a hexagonal Ru(0001) surface superimposed by the reciprocal unit mesh (b_1^*, b_2^*) of Pt-cluster as indicated by the dashed line where the reciprocal unit mesh of Pt is no longer matching with the substrate unit mesh, (c) Schematic drawing for 2D adlayer and 3D clusters of Pt deposit on Ru(0001).

position through short immersion into the Pt^{4+} containing $HClO_4$ solution. Intensity modulations along the (10) and (11) reflection streaks are discernible which are attributed to the overlap with scattering intensity from the Pt overlayer, since no such effect is visible with the Pt free sample if compared with Figs. 2a and 2b. Closer inspection reveals that Pt-reflections overlap with Ru-substrate reflections of both the [0110] and [1120] azimuths, implying that the reciprocal lattice vectors b_1^*, b_2^* from the Pt overlayer coincide with the reciprocal lattice vectors a_1^*, a_2^* from the substrate as illustrated in Fig. 3a. No further reflections except those arising from the substrate were observed upon azimuthal rotation of the electrode. This indicates that a non-rotated Pt overlayer was growing on the Ru(0001) surface, that means the reciprocal unit cell of the overlayer matches with that of the substrate surface. Hence in real space the formation of a Pt(111) plane coincident with the Ru(0001) surface with both exhibiting the same hexagonal unit mesh has to be inferred, as sketched in Fig. 3c.

More prolonged immersion into the Pt^{4+}-containing solution produced an electrode surface covered by three-dimensional Pt clusters: Inspection of the RHEED patterns reproduced in Figs. 2e and 2f reveal the existence of 3D-reflection spots apart from the known reflection streaks from the 10 or 11 beams. The reciprocal lattice length of the 3D-reflection near the 11-beam is $0.723\ \text{Å}^{-1}$. This agrees with the 220 reflection of Pt crystallites ($0.7209\ \text{Å}^{-1}$), but not with the 11-beam of the Ru substrate ($0.739\ \text{Å}^{-1}$). Moreover, the separation between spots along the 00 and 11 beams amounts to $0.443\ \text{Å}^{-1}$ which corresponds to the reciprocal of the separation $d_{111} = 2.26\ \text{Å}$ between neighboring (111) planes of Pt. It is thus concluded that now Pt clusters have grown with their (111) plane parallel to the Ru(0001) surface, but exhibiting some lattice mismatch: The [011] row spacing of the Pt(111) plane is about 2% larger than the [1120] row spacing of the Ru(0001) substrate. From the diameter of the 3D RHEED spots a mean cluster size of about 3 nm is derived.

The presented results demonstrate that spontaneous deposition of Pt on Ru(0001) leads at first to pseudomorphic growth, which may take place if the surface free energies of the film γ_f, the interface γ_{in}, and the substrate γ_s, fulfill the condition: $\Delta\gamma = \gamma_f + \gamma_{in} - \gamma_s < 0$ [13–15]. With growing film thickness, however, the increasing lattice strain causes also an increase of γ_{in} so that $\Delta\gamma > 0$ and 3D-crystals are forming. It has to be emphasized that both the 2D- and 3D growth modes of Pt on Ru(0001) could be achieved by spontaneous deposition from solution at room temperature. These results were obtained after treating the clean Ru(0001) surface by a potential sweep between -0.2 and 0.85 V in 0.1 M $HClO_4$ for characterization of the state of the surface prior to Pt deposition. In contrast, no spontaneous Pt deposition on Ru(0001) was reported in [6], where the Ru electrode was first immersed into H_2SO_4, pure water or 0.1 M $HClO_4$ for more than 1 min. The reason for the contradictory results is not yet clear.

An alternative route consists in electrochemical deposition by cycling the potential between -0.2 and 0.3 V in $PtCl_6^{-2}$ containing $HClO_4$ solution. The corresponding cyclovoltammograms (CV) showed that the current density for hydrogen adsorption/desorption increased significantly with the number of cycles. The same holds for the Pt surface concentration as monitored by Auger electron spectroscopy (AES). The data reproduced in Fig. 4 demonstrate that the Ru peaks from the clean Ru(0001) electrode (Fig. 4a) are strongly suppressed by electrodeposition while an intense Pt peak appears (Fig. 4c). A thin overlayer formed by spontaneous deposition is, on the other hand, characterized by Ru and Pt signals of comparable intensities (Fig. 4b).

A RHEED pattern recorded from a sample after 4 cycles of Pt electrodeposition is reproduced in Fig. 2g. It exhibits only 3D-reflection spots from Pt, while the reflection streaks from the Ru substrate are no longer discernible. From the widths of the spots an average cluster size of about 3 nm is derived. In contrast, the data from the sample prepared by spontaneous deposition (Figs. 2e and 2f) exhibited still Ru-diffraction streaks, apart from Pt 3D-reflections. This suggests that in this case still flat Ru patches exist be-

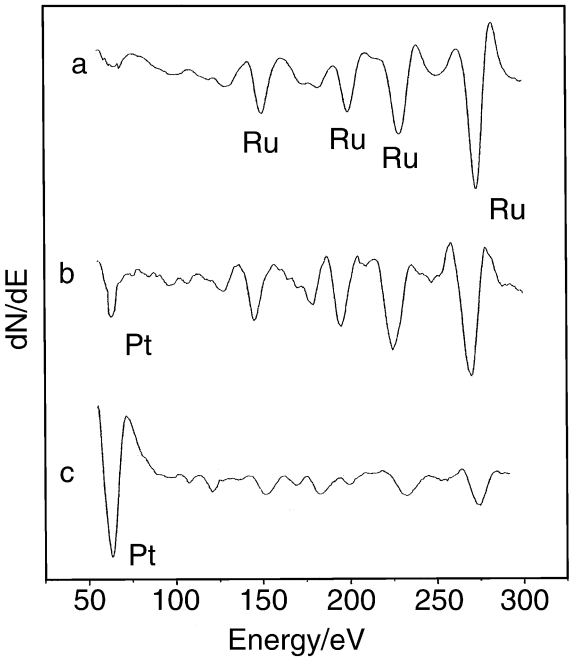

Fig. 4. Auger electron spectra: (a) for a clean Ru(0001) surface after argon ion sputtering and annealing under UHV conditions, (b) for a Ru(0001) electrode covered with a Pt adlayer by spontaneous deposition, (c) Ru(0001) electrode with Pt clusters formed by electrodepostion.

tween the Pt clusters, which conclusion will be supported by scanning electron microscopy (SEM) data to be shown below.

At last the possibility of alloy formation will be briefly addressed. If the 3D spots would be due to Pt-Ru alloys with varying composition, then – according to Vegard's rule [16] – the lattice constant would be expected to vary with the number of cycles of Pt electrodeposition. No change in the reciprocal lattice distance of the diffraction spots was observed, so that this possibility can be ruled out. The formation of a PtRu surface alloy was, however, observed after deposition of 0.4 ML of Pt onto Ru(0001) at 310 K followed by annealing at 1200 K [17]. RHEED was, for example, also able to detect the formation of a surface alloy of Cu/Au(111) associated with an 3%–4% increase of the reciprocal lattice separations between the Au substrate reflections [18].

Finally the morphology of the Ru surface after Pt deposition was characterized by SEM. A representative image obtained after 9 cycles of electrodeposition is reproduced in Fig. 5. The deposit consists of Pt-clusters with diameters between 2 and 10 nm with varying mutual separation ranging from 3 to 40 nm. The corresponding Auger electron spectrum is reproduced in Fig. 4c. It exhibits the characteristic Pt signal at 64 eV, while the Ru peaks are suppressed in intensity but still discernible. The morphology of the sample whose image is reproduced in Fig. 5 is rather similar to that probed by STM as reported for spontaneous Pt deposition [6]. However, in the latter case the surface distribution of Pt clusters was more dense and covered almost the whole surface area. This difference might be due to different deposition times and/or an effect by the supporting electrolyte containing strongly adsorbing sulfate ions in [6].

By reducing the number of electrodeposition cycles the SEM images indicate larger separations between the clusters, while their mean diameter remains essentially unaltered. On the other hand, more extended deposition caused about 80% of the Ru surface to become covered by Pt clusters with 2–8 nm diameter, where in AES the Ru signals largely disappeared.

It should be mentioned that both SEM and STM [6] essentially enable analysis of the mean cluster size and mutual separation, but not of their orientation with respect to the substrate. On the other hand, this can be readily achieved by RHEED (cf. Fig. 3c), together with determination of the unit mesh of the 2D-adlayer (cf. Fig. 3a).

Finally, the electrocatalytic properties of the Ru(0001) electrodes covered to about 80% by Pt deposits were probed by cyclic voltammetry (CV). The data taken in 0.1 M $HClO_4$ solution are shown in Fig. 6a. They exhibit marked differences in the range of hydrogen adsorption/desorption if compared with the behavior of a pure Ru(0001) surface. The profile of the CV from the modified electrode is very similar to that for a polycrystalline Pt electrode in the same electrolyte [19, 20]. The current density for hydrogen adsorption/desorption increases with the number of electrodeposition cycles, while the reduction peak at 0.25 V, typical for OH desorption at the Ru(0001) surface, decreases. After subtracting the contribution to the charge for H-adsorption on the Pt free Ru

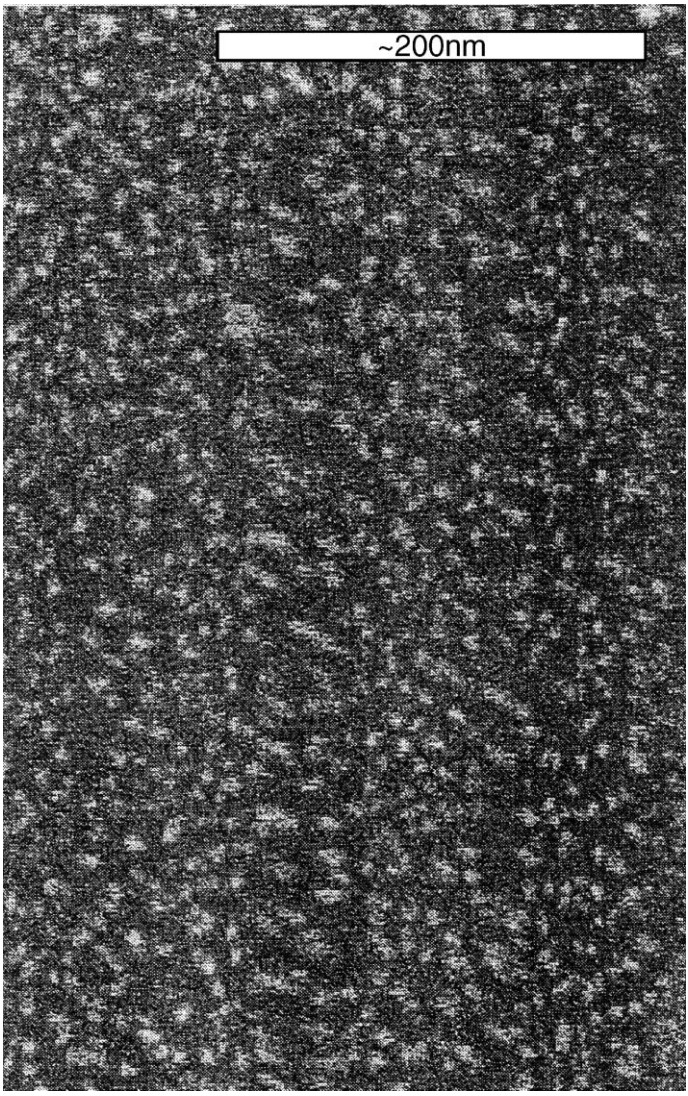

Fig. 5. Scanning electron microscopy (SEM) image for a Ru(0001) electrode after electrodeposition of Pt (Primary electron energy 25 keV).

electrode (full line), an enhanced charge of about 320 $\mu C/cm^2$ is derived for this quantity with the Pt-modified surface. This reflects an increase of the density of H-adsorption sites on the Pt cluster surfaces to about 2×10^{15} cm^{-2}. The charge associated with H-chemisorption on a flat Ru(0001) surface is 120 $\mu C/cm^2$ [24], while that on a flat Pt(111) surface amounts to 240 $\mu C/cm^2$.

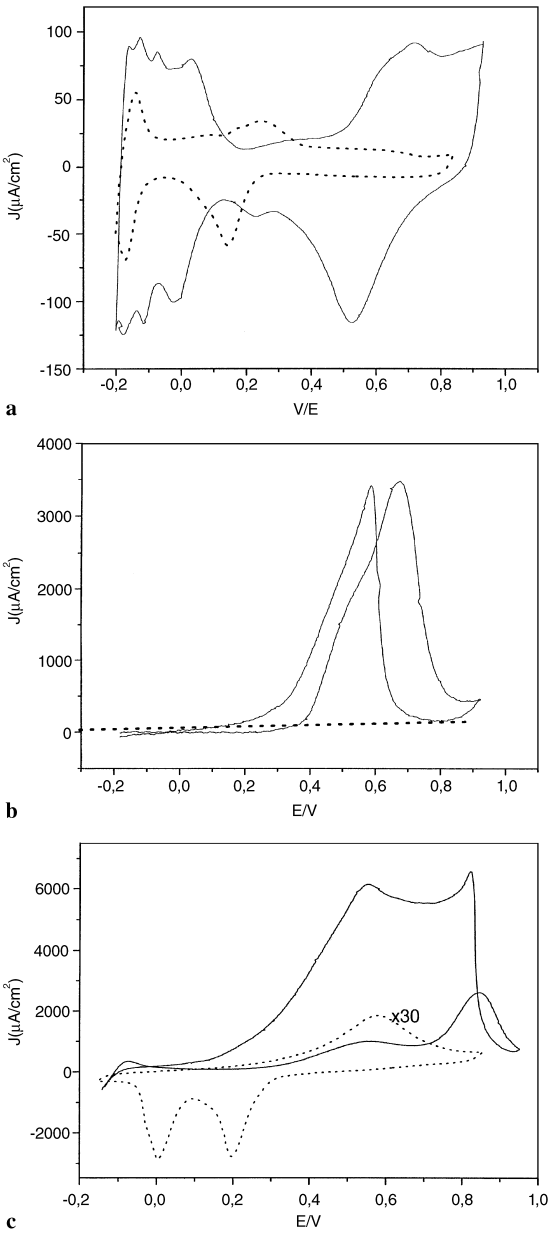

Fig. 6. Cylic voltammogram (CV) data recorded with a scan rate of 50 mV/s: (a) Ru(0001) electrode (broken line) and Ru surface covered by Pt clusters (full line) in 0.1 m $HClO_4$ solution, (b) Ru(0001) electrode (broken line) and Ru surface covered to 80% by Pt clusters (full line) in 0.1 M $HClO_4$ + 0.1 M CH_3OH, (c) Ru(0001) electrode (broken line) and Ru surface covered to 80% by Pt clusters (full line) in 0.1 M $HClO_4$ + 0.1 M HCOOH.

The latter value corresponds to an adatom density of about 1.5×10^{15} cm^2, being equivalent to 1 H atom per unit mesh [21–23]. The number for the Pt-modified Ru surface is even larger, presumably because of enhanced surface roughness.

The data for the electrocatalytic activity towards methanol or formic acid oxidation exhibit even more dramatic differences between the pure and Pt-modified Ru(0001) electrodes. Only representative examples will be shown here, while a full account will be given elsewhere [25]: As can be seen from Fig. 6b, pure Ru(0001) exhibits practically no activity in CH_3OH electrooxidation (broken line), while a marked oxidation peak is apparent with the surface covered to about 80% by Pt clusters (full line). It is noteworthy that the maximum of methanol oxidation current is ca. 3500 μA/cm^2 detected on the former electrode in a 0.1 M CH_3OH solution (see Fig. 6b) which is substantially higher than that found on a rough Pt(111) ($\approx$ 1500 μA/cm^2) [25] and the Pt-Ru bulk alloy surface ($\approx$ 900 μA/cm^2) [26] in a 0.05 M CH_3OH solution [26]. The latter exhibits even much higher activity than Pt(111) with Ru islands grown at 300 K [27]. Similarly, the current density associated with HCOOH electrooxidation on Ru(0001) (60 μA/cm^2) is enhanced by a factor of about 100 with the Pt-modified electrode as reflected by Fig. 6c.

Acknowledgement

The technical assistance by Mrs. G. Weinberg in obtaining the SEM images is gratefully acknowledged.

References

1. M. T. Keif and W. F. Egelhoff, Jr., Phys. Rev. B **47** (1993) 10 785.
2. H. A. Gasteiger, N. Markovic, P. N. Ross, and E. J. Cairns, J. Electrochim. Acta **39** (1994) 1825.
3. W. Chrzanowski and A. Wieckowski, Langmuir **14** (1998) 1967.
4. W. F. Lin, M. S. Zei, M. Eiswirth, G. Ertl, T. Iwasita, and W. Vielstich, J. Phys. Chem. B **103** (1999) 6968.
5. R. Ianniello, V. M. Schmidt, U. Stimming, J. Stumper, and A. Wallaw, Electrochim. Acta **39** (1994) 1863.
6. S. R. Brankovic, J. McBreen, and R. R. Adzic, J. Electroanal. Chem. **503** (2001) 99.
7. W. Chrzanowski, H. Kim, and A. Wieckowski, Catal. Lett. **50** (1998) 69.
8. K. A. Friedrich, K. P. Geyerz, A. Marmann, U. Stimming, and R. Vogel, Z. Phys. Chem. **208** (1999) 137.
9. M. J. Llorca, J. M. Feliu, A. Aldaz, and J. Clavilier, J. Electroanal. Chem. **376** (1994) 151.
10. G. Q. Lu, A. Crown, and A. Wieckowski, J. Phys. Chem. B **103** (1999) 9700.
11. G. Lehmpfuhl, Y. Uchida, M. S. Zei, and D. M. Kolb, in *Imaging of Surfaces and Interfaces*; Frontiers of Electrochemistry, ed. by J. Lipkowski and P. N. Ross, Vol. 5, Wiley-VCH, Weinheim, Germany (1999) p. 57.

12. W. F. Lin, M. S. Zei, Y. D. Kim, H. Over, and G. Ertl, J. Phys. Chem. B **104** (2000) 6040.
13. J. A. Rodriguez, Surf. Sci. Rep. **24** (1996) 223.
14. E. Bauer and J. H. van der Merwe, Phys. Rev. B **33** (1986) 3657.
15. L. Z. Mezey and J. Giber, Jpn. J. Appl. Phys. **21** (1982) 1569.
16. H. Glocker, *Materialprüfung mit Roentgenstrahlen*, Springer-Verlag, Berlin/Göttingen/Heidelberg (1958).
17. F. Buatier de Mongeot, M. Scherer, B. Gleich, E. Kopatzki, and R. J. Behm, Surf. Sci. **411** (1998) 249.
18. Y. Nakai, M. S. Zei, D. M. Kolb, and G. Lehmpfuhl, Ber. Bunsenges. Phys. Chem. **88** (1984) 340.
19. H. Hachkar, T. Napporn, J. M. Leger, B. Beden, and C. Lamy, Electrochim. Acta **41** (1996) 2721.
20. M. E. Gamboa-Aldeco, E. Herrero, P. S. Zelenay, and A. Wieckowski, J. Electroanal. Chem. **348** (1993) 451.
21. P. N. Ross, Surf. Sci. **102** (1981) 463.
22. K. Al. Jaaf-Golze, D. M. Kolb, and D. Scherson, J. Electroanal. Chem. **200** (1986) 353.
23. A. T. Hubbard, R. M. Ishikawa, and J. Katekaru, J. Electroanal. Chem. **86** (1978) 271.
24. W. B. Wang, M. S. Zei, and G. Ertl, Phys. Chem. Chem. Phys. **3** (2001) 3307.
25. T. Lei, M. S. Zei, and G. Ertl, to be published.
26. N. M. Markovic, H. T. Gasteiger, P. N. Ross, X. Jiang, I. Villegas, and M. J. Weaver, Electrochim. Acta **40** (1995) 91.
27. H. Hoster, T. Iwasita, H. Baumgärtner, and W. Vielstich, Phys. Chem. Chem. Phys. **3** (2001) 337.